UNIVERSITY OF PARDUBICE

FACULTY OF CHEMICAL TECHNOLOGY

Department of Graphic Arts and Photophysics

Tomáš Halenkovič

Chalcogenide thin films

Theses of the Doctoral Dissertation

Pardubice 2019

Study program: Chemistry and Technology of materials

Study field: Surface engineering

Author: Tomáš Halenkovič

Supervisor: prof. Ing. Petr Němec, PhD

Co-supervisor: doc. Virginie Nazabal, Dr.

Year of the defence: 2019

References

HALENKOVIČ, Tomáš. *Chalcogenide thin films*, 2019. 126 pages. Dissertation thesis (PhD.). University of Pardubice, Faculty of Chemical Technology, Department of Graphic Arts and Photophysics. Supervior Prof. Ing. Petr Němec, PhD. Co-supervisor doc. Virginie Nazabal, Dr.

Abstract

This thesis is focused on study of amorphous thin films of ternary Ge-Sb-Se and Ga-Sb-Se systems fabricated by co-sputtering technique for their potential applications in the field of nonlinear optics. General quality by means of morphology and topography, linear and non-linear optical properties and local structure of fabricated films depending on the composition are discussed. The limitation of these materials may lie in their photosensitivity under the near-bandgap light irradiation. Therefore, this aspect of co-sputtered thin films was also studied. In the frame of the thesis, optical properties and structure of quaternary Ge-Sb-Se-Te thin films fabricated by RF sputtering as a potential alternative to ternary systems were also studied.

Abstrakt

Práce se zabývá studiem tenkých amorfních vrstev ternárních systémů Ge-Sb-Se a Ga-Sb-Se připravených technikou magnetronového naprašování za simultánního použití několika terčů, pro jejich potenciální aplikace v nelineární optice. Je diskutována obecná kvalita ve smyslu morfologie a topografie, lineární a nelineární optické vlastnosti a struktura připravených vrstev v závislosti na složení. Omezení těchto materiálů může spočívat v jejich citlivosti na světlo blízké energii jejich optické šířce zakázaného pásu energií. Byl proto studován i tento aspekt. V rámci práce byly také studovány optické vlastnosti a struktura kvaternárních tenkých vrstev Ge-Sb-Se-Te připravených magnetronovým naprašováním.

Keywords

amorphous chalcogenides, sputtering, amorphous thin films, optical properties, structure

Keywords

amorfní chalkogenidy, naprašování, amorfní tenké vrstvy, optické vlastnosti, struktura

1. Introduction

Chalcogenide glasses and amorphous thin films are non-crystalline materials based on the elements of chalcogens (*i.e.* S, Se and Te) accompanied with other elements such as Ga, Ge, As, In, Sb *etc.* [1]. These materials have been widely studied since the 1950s [2].

In the form of bulks, they have often restricted use due to their limiting thermal and mechanical properties [3]. The limiting mechanical properties of chalcogenides relative to the rather strong oxide glasses came from the difference in the atomic bonding. Oxide glasses have strong covalent and ionic bonds forming the three-dimensional network, while chalcogenides have weak covalent bonds between two-fold coordinated chalcogen atoms forming a back-bone chain with cross-linking provided by 3- or 4-fold coordinated group 14 and group 15 atoms. The chains are interconnected by weak Van der Waals forces [3]. Therefore, in terms of atomic structure, chalcogenide glasses may be characterized as being between oxide glasses having the three-dimensional networks and organic polymers possessing one-dimensional chain structures [4, 5]. However, the good sharping ability of chalcogenide glasses enables its use in the form of fibres or thin films [6].

Chalcogenide glasses and amorphous thin films possess large number of unique properties, which make them incomparably interesting in many different fields.

First, due to the low phonon energies, they have the broad transmission window from visible to infrared (IR) [7]. The useful range of IR transmission of impurity-free chalcogenide glasses is ~0.6–11.5 μm for sulphides; ~1–15 μm for selenides and ~2–20 μm for tellurides [8]. Thus, chalcogenide glasses found their application in the field of optical sensors and IR fibre-optic devices [9, 10].

Moreover, low phonon energy of chalcogenides makes them suitable hosts for rare earth (RE) elements due to the low probability of multiphoton relaxation between RE^{3+} energy levels. The typical RE dopants are Pr^{3+}, Dy^{3+} or Tm^{3+} in near-infrared spectral range and Pr^{3+}, Dy^{3+}, Er^{3+}, Ho^{3+} or Tm^{3+} in the middle IR domain [11]. Potential applications of RE doped chalcogenide glasses include fabrication of fibre amplifiers for telecommunication and fibre lasers [12].

Furthermore, the advances in the signal processing such as all-optical switching operating typically on the picosecond time scales, requires materials with the high optical nonlinearities [13]. Chalcogenide glasses exhibit of about two orders of magnitude higher nonlinear refractive index when compared with oxide glasses [14]. Moreover, second-harmonic generation in optically isotropic chalcogenide glasses may occur [15]. When the optical pulse travels through the medium with high nonlinear refractive index, it becomes distorted in phase (self-phase modulation) and in envelope shape (self-steepening) [16]. The former is responsible for supercontinuum (SC) generation in various materials. SC generation in chalcogenide fibres and waveguides in Mid-IR region seems to have a great potential [17, 18]. Finally, high "Kerr-like" nonlinearities in combination with proper dispersion may lead to solitary wave formation and propagation in chalcogenide glasses [19]. Thus, amorphous chalcogenides are of interest in the wide spectrum of possible applications such as high-speed optoelectronic devices and photonic switching [20].

Perhaps the most striking property of non-crystalline chalcogenides is their photosensitivity, which includes numerous phenomena caused by the electromagnetic radiation [21].

The thin films studied in the frame of this work come from Ge-Sb-Se, Ga-Sb-Se and Ge-Sb-Se-Te systems. The choice of studied systems was made based on below described reasons.

Due to the presence of arsenic in classical binary chalcogenides (As_2S_3, As_2Se_3), which is highly toxic in its elemental form, arsenic-based chalcogenides are supposed to be environmentally improper for some applications [22]. These include (bio)chemical sensors that are likely to be discarded after their use [23]. Thus, exploiting germanium as an alternative glass network former, with respect to required wide transparency in mid-IR region, high (non)linear refractive index and glass-forming ability, the Ge-Se system should be advantageous when compared to Ge-S or Ge-Te [24, 25]. Moreover, in contrast with arsenic-based chalcogenides, four-fold coordinated germanium atoms spatially sustain the glass network resulting in higher glass-transition temperature (T_g) and improved mechanical properties, *i.e.* network rigidity, strength and hardness [14]. Covalent glasses of ternary Ge-As-Se and Ge-Sb-Se systems have been recently widely studied due to relatively large glass-forming domain and good physical and mechanical properties in comparison with classical binary chalcogenide compounds. Despite the particular attractivity of Ge-As-Se system having greater glass-forming ability when compared to Ge-Sb-Se system, the introduction of antimony in the glass network provides higher polarizability increasing (non)linear refractive index and reduced photosensitivity [26] offering an interesting option for the applications in the field of nonlinear optics [27-29].

Recently, germanium-free chalcogenide system of Ga-Sb-Se has been investigated by Lecomte *et al.* for the potential night-vision applications [30]. Furthermore, Sb-rich Ga-Sb-Se co-sputtered films are considered to be a potential replacement of Ge-Sb-Te (GST) for phase-change memories having higher thermal stability, smaller density change and higher crystallization speed when compared to GST [31]. The glass-forming domain of Ga-Sb-Se system is relatively large when compared to the Ge-Sb-Te. Potential application of Ga-Sb-Se amorphous thin films in the field of nonlinear optics should be also considered. Finally, this system may be also interesting for luminescence studies due to the good solubility of rare-earth elements in gallium-containing chalcogenide glasses/films. However, the photo-sensitivity of Ga-Sb-Se glasses/thin films has not been investigated until now.

The last system investigated in the frame of this thesis is Ge-Sb-Se-Te quaternary with Te content of 10 and 15 atomic percent. It has been shown by Sharma *et al.* that the substitution of selenium by tellurium leads to the increase in (non)linear refractive index making these chalcogenide glasses potential candidates for integrated optics, ultrahigh-bandwidth signal processing and infrared optical sensor applications [32]. High selenium concentration in Ge-Sb-Se-Te quaternary alloys is expected to increase the glass-forming domain.

2. Experimental procedures

Some of the key techniques for the present work are described in the following subchapters including the unique physical vapor deposition technique of co-sputtering. Ubiquitous characterization techniques of spectroscopic ellipsometry and atomic force microscopy used in the frame of this thesis are listed. Finally, the technique of beam-self trapping technique which was exploited during the thesis is also briefly discussed.

2.1. Co-sputtering

Sputtering employing multiple cathodes (co-sputtering) brings the advantage of adjustable electrical power ratio applied on individual cathodes which enables to obtain thin films with various compositions. It is also an efficient deposition method to fabricate amorphous thin films whose composition is out of glass-forming region of the system under study. This makes co-sputtering cost-effective for compositional dependencies' studies of materials' properties. The schematic representation of three cathode geometry co-sputtering is shown in the figure 2-1.

In spite of obvious advantages of co-sputtering, this is not commonly used technique for amorphous chalcogenide thin films fabrication. Recently, RF magnetron co-sputtering technique was used for the compositional dependencies studies of various properties of chalcogenide amorphous thin films. Lin *et al.* studied photo-induced structural changes in co-sputtered Ge-Sb-Se films using $GeSe_2$ and Sb sputtering targets [33]. Photo-induced effects in the same system (however with higher selenium content) were studied by Halenkovič *et al*. In their work, they used targets with compositions $GeSe_2$, Sb_2Se_3 and $Ge_{28}Sb_{12}Se_{60}$ [25]. Compositional dependence of crystallization and structural stability in Se-poor co-sputtered Ge-Sb-Se films from $Ge_{20}Sb_{15}Se_{65}$ (or $Ge_{28}Sb_{12}Se_{60}$) and Sb(Ge) targets were studied by Wang *et al.* [34]. Optical properties of In-Ge-Se thin films co-sputtered from $GeSe_2$ and In targets were studied by Chen *et al.* [35].

Co-sputtering was also used for the studies of phase-change kinetics of amorphous $Ge_2Sb_2Te_5$ (GST). Cho *et al.* used co-sputtering technique for "doping" of GSTs by bismuth and aluminium using GST and $Ge_2Bi_2Te_5$ (or Al) targets [36]. Phase-change transition characteristics of bismuth and tin "doped" GST thin films for phase-change random access memory were studied by Park *et al.* [37]. In their work GST, Bi and Sn targets were employed.

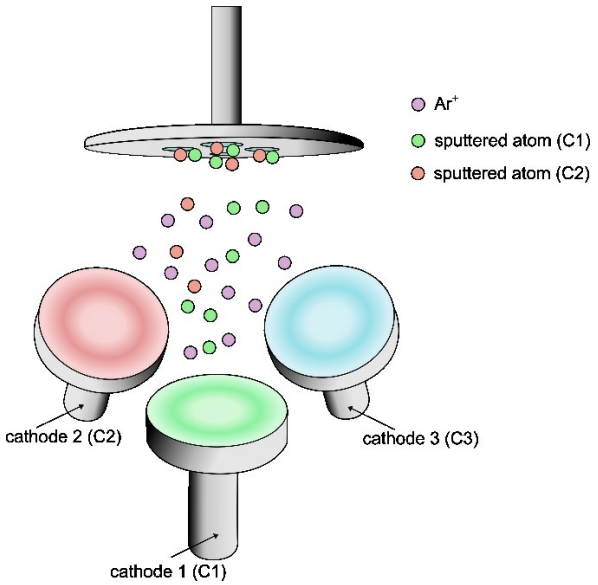

Fig. 2-1 Schematic representation of three-cathode geometry of co-sputtering technique with electrical power applied on two cathodes (C1 + C2).

2.2. Spectroscopic ellipsometry

Ellipsometry is based on the measurement of the change of the polarization of the light as it interacts with the sample. Two ellipsometric parameters, ψ and Δ, are directly obtained from ellipsometry measurement [38]. Spectroscopic ellipsometry is a very sensitive technique which is routinely used to measure thickness and optical constants of dielectric, semiconductor and metal thin films. It enables the evaluation of the complex dielectric function, $\varepsilon = \varepsilon_1 + i\,\varepsilon_2$, which is related to the refractive index, n, and extinction coefficient, k, $\varepsilon = (n+ik)^2$, through ψ and Δ. The determination of complex dielectric function enables the investigation of the electronic structure of material, which is related to the joint density of states for interband absorption [39].

2.3. Amplitude modulated atomic force microscopy (AM-AFM)

Atomic force microscopy seems to be powerful tool to examine the topographical properties of the surface of dielectric thin films such as chalcogenides. Lacking the electrons on the surface of such films, this scanning probe microscopy technique uses the special probe (cantilever) usually having silicon or silicon nitride tip with the reflective backside coating. The attractive/repulsive forces between the cantilever tip and the scanned surface cause the deflection of the tip, which is detected using laser diode and position photodetector (quadrant photodiode). Perhaps most often used AFM technique is amplitude modulated atomic force microscopy (AM-AFM). In AM-AFM, the tip of the cantilever is not in the contact with the sample; however intermitted contact between the tip and the sample may occur. For this reason, AM-AFM is sometimes called “tapping mode” or “semi-contact mode”, [40].

Cantilever being “exited” using piezo close to its resonant frequency is approached to the sample surface until the set value of amplitude deflection (SetPoint) is achieved. Surface roughness of the film is then recorded by means of deviation from the SetPoint

value. Feedback loop of the Z-signal returns the cantilever to the initial SetPoint value immediately, so the lateral information about the sample surface roughness is obtained [41]. The scheme of AM-AFM is shown in figure 2-2.

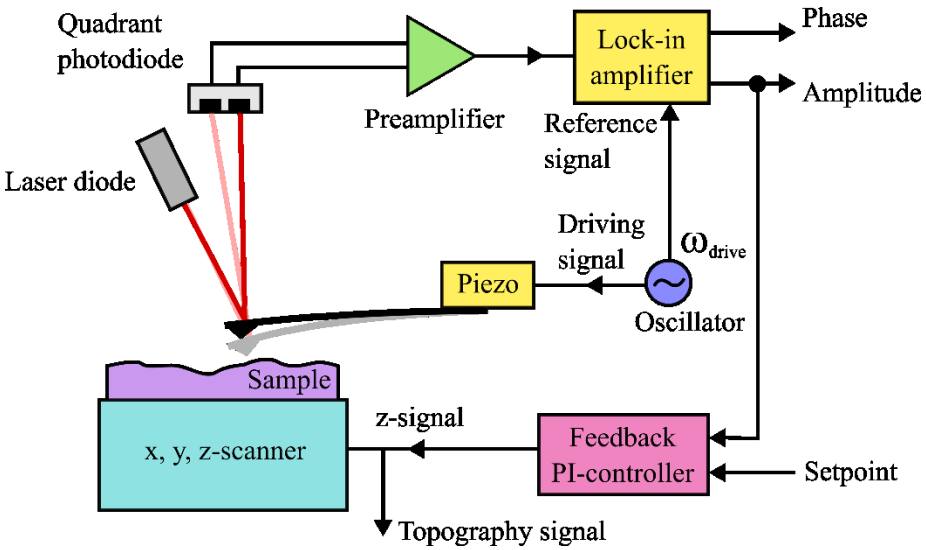

Fig. 2-2 AM-AFM detection scheme with lock-in amplifier for the detection of deviation of the oscillation amplitude from the SetPoint value – redraw from Voigtländer [41].

2.4. Beam self-trapping technique

Beam self-trapping technique is an experimental technique suitable for the measurements of nonlinear optical properties of thin films. It is based on the analysis of the spatial light beam distribution propagating in the slab waveguide. In such measurement the laser beam reshaped to an elliptical spot by cylindrical lens and focused by × 40 microscope objective enters the waveguide. The light is coupled using the combination of half-wave plate and polarizer. Beam distribution at the output of the waveguide is then monitored using IR camera with × 10 microscope objective [42].

In the linear regime, the input bean being narrow (*i.e.* few tens of micrometres) enlarges due to the diffraction along few millimetres propagation distance. In nonlinear regime, the diffraction is modified due to either self-focusing or self-defocusing [43]. Considering both linear and nonlinear absorption the optical beam propagation is modelled by the nonlinear Schrödinger equation [44]:

$$\frac{\partial E}{\partial z} = -\frac{\alpha}{2} - \frac{\beta}{2}|E^2|\,E + iK_0 n_2 |E^2|\,E \qquad \text{Eq. 2-1}$$

where electric field E is related to the intensity by $I = [E^2]$. K_0 is the propagation constant in the medium. Nonlinear refractive index n_2 is deduced by analysis of the output beam profile modification as a function of the injected light power [43].

Self-trapped optical beam that propagates in a nonlinear medium without diffraction is called optical spatial soliton [45]. Plasmon-soliton coupling in planar waveguides was recently demonstrated experimentally by Kuriakose *et al.* [46]. In their experiment, the

metal-dielectric structure consists of medium with Kerr nonlinearity placed on lower refractive index medium with a thin dielectric layer and metallic film deposited on top. Specifically, the medium with Kerr nonlinearity is amorphous chalcogenide film ($Ge_{28.1}Sb_{6.3}Se_{65.6}$) of thickness of 3 μm deposited by RF sputtering technique on thermally oxidized silicon substrate. Dielectric layer deposited on the top of the chalcogenide waveguide is silicon oxide with the thickness of 10 nm. Finally, the metallic film is 30 nm thick gold layer [46]. Beam self-trapping is considered to have a great potential as a characterization technique of nonlinear optical properties of thin films. When compared to other available techniques (*e.g.* z-scan technique) the influence of the substrate is negligible. Besides that, it enables the characterization of very thin films [42].

3. Results and Discussion

Optical properties of co-sputtered Ge-Sb-Se, Ga-Sb-Se and sputtered Ge-Sb-Se-Te thin films in the wavelength region of 300-2300 nm were investigated using variable angle spectroscopic ellipsometry (VASE, J. A. Woollam Co., Inc., Lincoln, NE, USA). For Ge-Sb-Se and Ga-Sb-Se thin films deposited on BK7 substrates, the data were collected at the angles of incidence of 50, 60 and 70° with 10 nm step. Three-layer model, consisting of substrate, actual amorphous chalcogenide thin film and simulated surface roughness (effective medium approximation consisting of 50 % of voids and 50 % of optical constants of film layer), was used for the determination of optical properties (*i.e.* optical bandgap and refractive index) and thickness. Imaginary part of dielectric function was fitted using Cody-Lorentz oscillator model. The data were fitted using WASE32 software. For the convenience the optical energy bandgap determined by VASE *via* CL model is referred to as E_g^{CL}.

Furthermore, optical bandgap was also determined from transmission-reflectance measurements in the range of 350-2500 nm employing Lambda 1050 spectrophotometer (Perkin-Elmer Inc., Waltham, MA, USA) or transmission measurements in the range of 180-3300 nm using spectrophotometer UV-3600 Plus (Shimadzu Co., Kyoto, Japan). Additionally to VASE, optical bandgap energy E_g^{opt}(hereinafter referred to as E_g^T) was obtained following Tauc approach [47] from energy dependence of $(\alpha\hbar\omega)^{1/2}$ by an extrapolation the linear part of the absorption edge curve found in the high absorption region ($\alpha \gtrsim 10^4$ cm^{-1}).

Generally, there is a good agreement between the values of E_g^{CL} and E_g^T, though the former is usually little bit higher. This can be reasonably explained when one compares the methodology of determination of optical bandgap values by these two methods [25].

For the investigation of optical properties of thin films from Ge-Sb-Se system, co-sputtering of pseudo-binary systems of $GeSe_2$-Sb_2Se_3, $GeSe_2$-$Ge_{28}Sb_{12}Se_{60}$, Sb_2Se_3-$Ge_{28}Sb_{12}Se_{60}$ and $GeSe_4$-Sb_2Se_3 were examined. Three commercial targets with following composition were selected: polycrystalline $GeSe_2$ (American Elements Corp., Los Angeles, CA, USA), polycrystalline Sb_2Se_3 (American Elements Corp., Los Angeles, CA, USA), glassy $Ge_{28}Sb_{12}Se_{60}$ (Vitron GmbH., Jena, Germany). $GeSe_4$ target was prepared by conventional melt-quenching technique. X-ray diffraction of bulky $GeSe_4$ taken in the range of 2θ from 5 to 90° (with 0.026° step) indicates that the melt-

quenched target is amorphous. The composition according EDS measurements is $Ge_{21.1}Se_{78.9}$ (± 1 at. %). The density measured at the room temperature (20 °C) was found to be 4.28 g.cm^{-3}. Finally, T_g was found to be 180 °C (at heating rate of 10 °C.min^{-1}) according the DSC measurements.

The sputtering depositions were performed at room temperature using MPE600 multi-chamber deposition system (Plassys-Bestek, Marolles-en-Hurepoix, France) with symmetrically arranged confocal deposition cluster consisting of three cathodes. The experimental conditions were held constant throughout all the depositions: background pressure $\leq 5 \times 10^{-7}$ mbar, Ar working pressure 5×10^{-3} mbar, Ar flow rate 75 sscm, with substrate holder rotation.

For the co-sputtering depositions from $GeSe_2$, Sb_2Se_3 and $Ge_{28}Sb_{12}Se_{60}$ targets, the electrical power on cathodes was chosen so the $P(C_x)+P(C_y)$ was always equal to 20 W. For the further investigation of $GeSe_4$-Sb_2Se_3 the maximum electrical power on $GeSe_4$ target was set to 12 W to minimize the damage of fragile target due to the erosion.

It should be noted that the morphology and the chemical composition was studied by scanning electron microscopy (SEM) with an energy-dispersive X-ray analyser (EDS, JSM 6400-OXFORD Link INCA, JEOL Ltd., Tokyo, Japan). For the evaluation of the chemical composition via EDS, L-lines were selected for all the constituting elements. Accelerating voltage used for SEM-EDS measurements was 10 kV.

The chemical composition of sputtered films obtained from $GeSe_2$, $GeSe_4$, Sb_2Se_3 and $Ge_{28}Sb_{12}Se_{60}$ was found to be close to the composition of targets in frame of EDS measurements uncertainty.

Despite relatively different deposition rates, the real chemical compositions of films deposited at 10/10 W were found to be close to its theoretical pseudo-binary counterparts $(C_x)_{50}(C_y)_{50}$. The real chemical composition of co-sputtered $GeSe_2$/Sb_2Se_3 10/10 W was found to be very close to an expected $(GeSe_2)_{50}(Sb_2Se_3)_{50}$, *i.e.* real composition $Ge_{12.3}Sb_{24.8}Se_{62.9}$ against theoretical $Ge_{12.5}Sb_{25}Se_{62.5}$. It is the case also for $GeSe_4$/Sb_2Se_3 10/10 W where the real composition is $Ge_{7.4}Sb_{24.5}Se_{68.1}$ against theoretical $Ge_{7.5}Sb_{25.0}Se_{67.5}$ in $(GeSe_4)_{50}(Sb_2Se_3)_{50}$ pseudo-binary. Similarly, for sample deposited from $GeSe_2$/$Ge_{28}Se_{12}Se_{60}$ 10/10 W, the real composition is $Ge_{30.6}Sb_{6.7}Se_{62.7}$ against $Ge_{30.7}Sb_{6.0}Se_{63.3}$. Finally, film deposited at the 10/10 W from Sb_2Se_3/$Ge_{28}Sb_{12}Se_{60}$ with composition $Ge_{11.2}Sb_{28.4}Se_{60.4}$ contains a small deficit of antimony when compared to its theoretical pseudo-binary counterpart $(Sb_2Se_3)_{50}(Ge_{28}Sb_{12}Se_{60})_{50}$ having composition $Ge_{10.5}Sb_{29.5}Se_{60.0}$. This shows only very small limitation of predictive approach of co-sputtered film composition. Thus, the perfect knowledge of deposition rate of individual targets, plasma characteristics, density and molecular weight of targets and films is necessary for predicting the chemical composition of co-sputtered films. However, the selenium content in the films is well maintained at given electrical power and argon working pressure [25].

Values of optical bandgap energy E_g^{CL} and refractive index at 1.55 μm are plotted in the ternary contour diagrams shown in the figure 3-1. The black dots correspond to the data points of each selenide thin films and the colored surfaces correspond to an interpolation between the data points. As seen, optical properties of co-sputtered films can be gradually tailored in terms of optical bandgap and refractive index. Furthermore, wide range of bandgap and refractive index is obtained by simple variation of electrical power on individual cathodes by co-sputtering technique. Values of E_g^{CL} and refractive index at 1.55 μm are found to cover the range between extreme values representing the

individual targets – *i.e.* 2.09 eV (n = 2.38) for $GeSe_2$, 1.97 eV (n = 2.44) for $GeSe_4$, 1.68 eV for $Ge_{28}Sb_{12}Se_{60}$ (n = 2.66) and 1.34 eV for Sb_2Se_3 (n = 3.34).

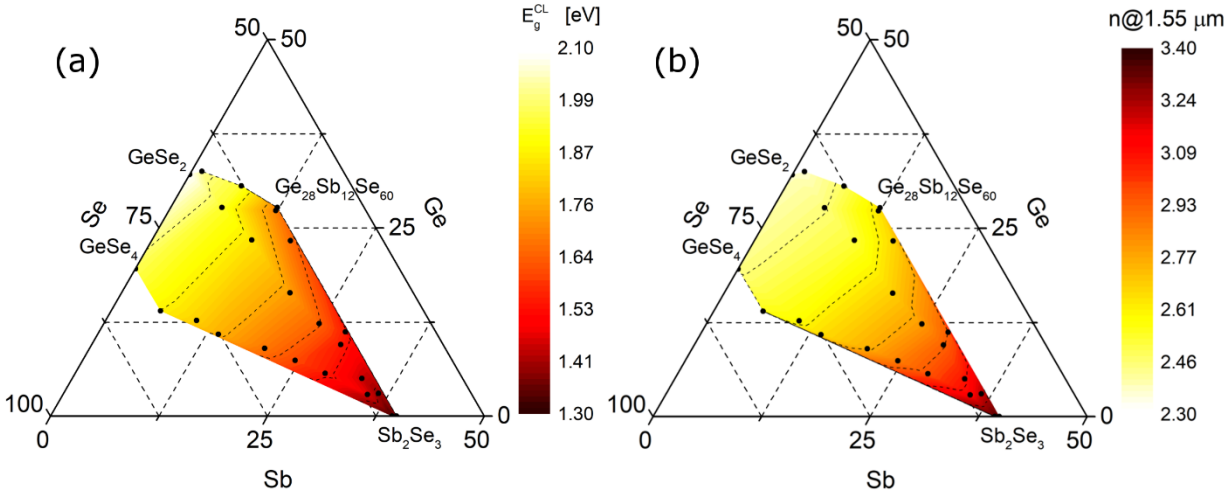

Fig. 3-1 Ternary contour diagrams showing the variation of optical bandgap energy **(a)** and refractive index **(b)** at 1.55 μm throughout the composition of Ge-Sb-Se co-sputtered thin films.

Co-sputtered thin films from the system Ga-Sb-Se were deposited using polycrystalline targets of Ga_2Se_3 and Sb_2Se_3. The deposition rate of Ga_2Se_3 was found to be only around 0.8 and 1.8 nm·min^{-1} at 10 and 15 W, respectively. Recalling estimated deposition rates for Sb_2Se_3, *i.e.* ~3.0 and 6.2 nm·min^{-1} for 10 and 15 W, respectively, it is obvious that no composition equal to the composition of pseudo-binary $(Ga_2Se_3)_{50}(Sb_2Se_3)_{50}$ (*i.e.* $Ga_{20}Sb_{20}Se_{60}$) can be achieved. The depositions were carried out in order to achieve acceptable thickness (at least 500 nm); however, due to the large difference in the deposition rate of the two targets and low deposition rate for Ga_2Se_3, it was not possible to use $P(C_x)+P(C_y)$ always equal to 20 W as for co-sputtered Ge-Sb-Se films. The morphology and the chemical composition was studied by SEM-EDS (TESCAN 5130SB, TESCAN, Brno, Czech Republic). Accelerating voltage used for SEM-EDS measurements was 10 kV.

The value of optical bandgap energy E_g^T of Ga_2Se_3 (E_g^{CL}= 1.92 eV) film is in a good agreement with the literature. Afifi *et al.* [48] reported the value of 2.06 eV for evaporated Ga_2Se_3 using Tauc extrapolation (E_g extracted from ellipsometry data). As expected, the increase of antimony content shifts the fundamental short-wavelength absorption edge towards the lower energies. Furthermore, the value of E_U corresponding to Urbach energy decreases from 160 ± 20 meV in Ga_2Se_3 film down to 76 ± 20 meV in $Ga_{7.6}Sb_{31.2}Se_{61.2}$. Therefore, it can be concluded that the values of E_u parameter decrease with increasing antimony content. Such 'sharpening' of absorption edge is apparent from the change in the slope of the absorption coefficient curves. This may indicate that the introduction of three-fold coordinated antimony induces the higher order in disordered films, possibly reducing the number of homopolar bonds such as Se–Se, Ga–Ga and selenium chains.

Thin amorphous Ge-Sb-Se-Te films were sputtered using the targets with the composition based on the Ge-Sb-Se glass previously described as 2S1G-Se4 by Olivier *et al.* corresponding to $(GeSe_2)_{70}(Sb_2Se_3)_{30}$ pseudo-binary ($Ge_{19.4}Sb_{16.7}Se_{63.9}$) [28]. This

particular composition was selected due to its suitability for nonlinear photonics devices applications [42]. Due to its good transparency in mid-IR region relative to sulphides, this composition is also suitable for the mid-IR sensors for the sea water pollution detection [49, 50]. In order to increase the refractive index, selenium was partially altered by tellurium in the amount of 10 and 15 atomic percent. Thus, these compositions will be referred to as 2S1G-Se4-Te10 and 2S1G-Se4-Te15 afterwards. Sputtering targets were prepared by conventional melt-quenching technique. X-ray diffraction patterns of bulky Ge-Sb-Se-Te taken in the range of 2θ from 5 to 90° (with 0.026° step) indicate that the melt-quenched targets are predominantly amorphous. The values of T_g for these compositions were found to be 244 and 231 °C (at heating rate of 10 °C.min^{-1}) respectively, according the DSC measurements. The decrease of T_g with increasing tellurium content is in a good agreement with recently published data for Tb^{3+} doped $Ga_5Ge_{20}Sb_{10}Se_{65-x}Te_x$ bulk glasses [51].

Increase of argon pressure during the deposition process seems to affect the optical properties represented by optical bandgap energy (E_g^{CL}) and refractive index obtained from VASE measurements. The MSE values of about ~1 confirm a good fit of the measured data by CL model. Considering the accuracy of the VASE measurements being ± 0.02 for E_g^{CL} and ± 0.01 for n, the most important changes were observed for the films deposited from 2S1G-Se4-Te10 target. With an increased argon pressure from 5×10^{-3} mbar to 10×10^{-3} mbar, the optical bandgap decreased by approximately ~0.1 eV. A considerable increase of refractive index connected with the increase of argon pressure was also observed: ~0.1 for samples deposited at 10 W, and 0.07 for samples deposited at 15 W. In the case of samples sputtered from 2S1G-Se4-Te15 target, the observed changes are the opposite, *i.e.* the bandgap energy was increased with increasing argon pressure accompanied with the decrease in refractive index. It should be noted that in sputtered Ge-Sb-Se thin films, the drop of the refractive index reflects morphology changes generated by increased argon pressure [9].

The nonlinear refractive index n_2 and two-photon absorption (2PA) coefficient β at the wavelength of 1.55 μm were calculated by Sheik-Bahae's formulae [52]. This approach was chosen for its relative simplicity when the linear refractive index dispersion and the optical bandgap are used. The dispersion curves and optical bandgap energies of thin films were obtained from the VASE data analysis. Taking in account the uncertainty of VASE measurements together with the mean absolute deviation from the Miller's rule, considered accuracy of these calculations in about ~13 %.

As seen in the figure 3-2, calculated data of nonlinear refractive index for all Ge-Sb-Se co-sputtered films are in a good agreement with data measured by Wang *et al.* who performed z-scan measurements at 1.55 μm within Ge-Sb-Se bulk glasses of thickness of ~2 mm [53]. Similarly, the values of n_2 are close to the data reported by Olivier *et al.* for bulk glasses of ~2 mm thickness measured by beam self-trapping technique at 1.55 μm [28]. The data reported by Kuriakose *et al.* for Ge-Sb-Se slab waveguides measured by the same technique at 1.55 μm [42] give a little bit higher values of n_2. Furthermore, calculated data given in figure 3-2 are in a good agreement with semi-empirical Miller's rule. Tichá and Tichý [54] reported some values of n_2 for bulk Ge-Sb-Se glasses calculated by generalized Miller rule corresponding to n_0 at $\lambda\rightarrow\infty$. Their data in esu units were converted to SI units in figure 3-2 by simple relationship $n_2[SI] = (40\pi/(cn_0) \cdot n_2[esu]$.

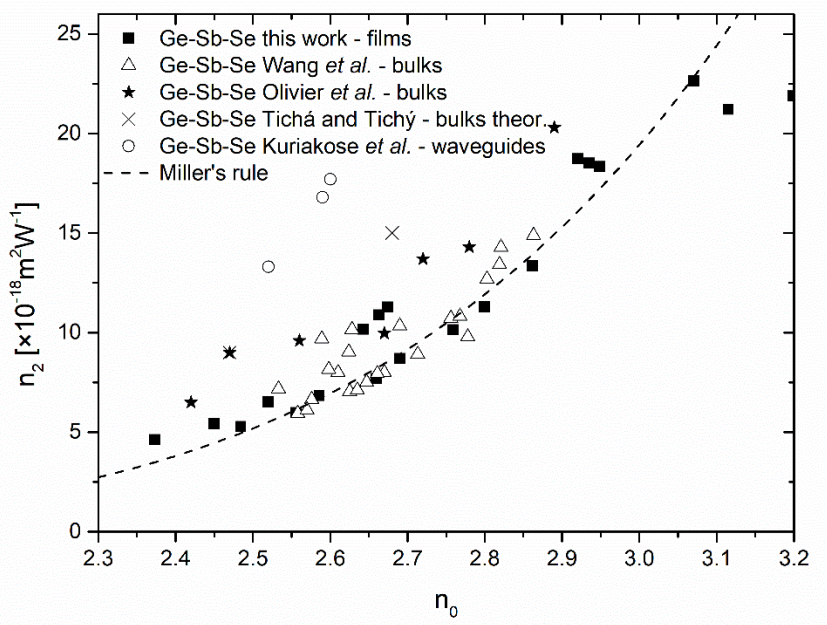

Fig. 3-2 Comparison of nonlinear refractive index n_2 at 1.55 μm of Ge-Sb-Se co-sputtered thin films calculated using Sheik-Bahae's model with experimental data taken from Wang *et al.* (z-scan measurements of bulk glasses with thickness of ~2 mm) at 1.55 μm [53], from Olivier *et al.* (beam self-trapping measurements of bulk glasses of ~2 mm) at 1.55 μm [28], from Kuriakose *et al.* (beam self-trapping measurements of Ge-Sb-Se slab waveguides) at 1.55 μm [42], theoretical values of n_2 (calculated by generalized Miller rule by Tichá and Tichý for Ge-Sb-Se bulk glasses) at $\lambda \rightarrow \infty$ [54] and semi-empirical Miller's rule.

In Ga-Sb-Se system, co-sputtered films corresponding to Ga_2Se_3-Sb_2Se_3 pseudo-binary were considered for nonlinear optics applications. The values of n_2 ranges from 5.50×10^{-18} m^2W^{-1} for antimony-free Ga_2Se_3 up to 2.09×10^{-17} m^2W^{-1} for the sample with composition $Ga_{7.6}Sb_{31.2}Se_{61.2}$. 2PA coefficient β for co-sputtered Ga-Sb-Se films reaches zero for samples having optical bandgap E_g^{CL} higher than 1.65 eV corresponding to sample with composition $Ga_{19.2}Sb_{17.5}Se_{63.3}$. The linear refractive index of this sample (n_0) at 1.55 μm is 2.80.

In the case of Ge-Sb-Se-Te system, the values of nonlinear refractive index are higher than those of Ge-Sb-Se system (~2.1-2.6 $\times$ 10^{-17} m^2W^{-1}). However, the low optical bandgap values E_g^{CL} lead to the high 2PA coefficient β which may reach more than ~30 $\times$ 10^{-11} $m \cdot W^{-1}$ for 2S1G-Se4-Te15 sputtered films. Unfortunately, this fact makes Ge-Sb-Se-Te films considerably ineffective for the applications in nonlinear optics at the telecommunication wavelengths.

The local structure of deposited films was studied using micro-Raman spectroscopy (LabRam HR800, Horiba Jobin-Yvon, NJ, USA) coupled with a ×100 microscope (Olympus, JP) with the excitation wavelength of 785 nm. In order to prevent the sample heating, neutral density filters were used to attenuate the laser intensity. The effect of thermal population at low wavenumbers was minimized by the reduction of Raman intensity defined in [55] as $I_{red}(\omega) = I_{meas}(\omega) \cdot \omega/[n(\omega) + 1]$, where $I_{meas}(\omega)$ represents the experimental Raman intensity at a frequency ω and $n(\omega)$ is the Bose-Einstein temperature occupation factor for the Stokes shift, given by $n(\omega) = (\exp[(\hbar\omega/k_BT) - 1])^{-1}$. Here, $\hbar$ is a reduced Planck constant, k_B is a Boltzman constant and T is a temperature. After the reduction, the spectra were normalized by

means of the division by the maximum value. The results of Raman spectra analysis are briefly discussed in the conclusion.

VASE was used for the determination of the optical bandgap energy and refractive index of thin films before (in as-deposited state) and after the irradiation. Photoinduced changes by means of optical bandgap change and the refractive index at 1.55 μm change are thus $\Delta E_g^{CL} = E_g^{CL}(irradiated) - E_g^{CL}(as-deposited)$ and $\Delta n = n(irradiated) - n(as-deposited)$ respectively.

Moreover, direct transmission measurements using portable spectrophotometer EPP 2000 (StellarNet Inc., Tampa, FL, USA) were carried out to quickly control the shift of the short-wavelength absorption edge during the irradiation.

For the experiments, the used light source is continuous-wave monochromatic diode-pumped solid state laser or laser diode of desired wavelength. The distance between the laser source and the sample is approximately 75 cm. In this path, the beam may be attenuated or reshaped if needed so the beam of the intensity of 150 $mW \cdot cm^{-1}$ (±10 %) is achieved. The sample is placed in the photo-kinetic cell under pure argon atmosphere in order to minimize the surface oxidation of the samples. All the samples were irradiated for 180 minutes.

For the irradiation, the laser source with the wavelength near the optical bandgap was chosen. Specifically, the penetration depth (1/α) of the source must be larger, but close to the film's thickness. In this work, appropriate light sources operating at 532 nm (2.33 eV), 593.5 nm (2.09 eV), 635 nm (1.95 eV), 656 nm (1.89 eV), 730 nm (1.70 eV), 785 nm (1.58 eV) and 808 nm (1.53 eV) were at the disposal. The results of photosensitivity studies of co-sputtered Ge-Sb-Se and Ga-Sb-Se are briefly summarized in the conclusion.

4. Conclusion

Magnetron co-sputtering technique allows a deep study of various properties throughout the composition in ternary amorphous chalcogenides [25]. It is also considered to be an efficient deposition method to fabricate amorphous thin films whose composition is out of glass-forming region of the system under study. In the frame of this thesis, optical properties, structure and photosensitivity of co-sputtered thin films of Ge-Sb-Se and Ga-Sb-Se systems were investigated. Furthermore, optical properties and the structure of sputtered thin films of Ge-Sb-Se-Te were studied.

Thin films of amorphous Ge-Sb-Se and Ga-Sb-Se fabricated by co-sputtering technique were found to be of good optical quality with surface roughness (RMS) typically around ~0.3 ± 0.2 nm and ~0.2 ± 0.1 nm respectively. The optical bandgap energies E_g^{CL} range 1.35-2.09 eV with corresponding refractive index ranging from 3.34 to 2.38 can be reliably covered in Ge-Sb-Se ternary system, when targets with compositions of Sb_2Se_3 (E_g^{CL} = 1.35 eV), $GeSe_2$ (E_g^{CL} = 2.09 eV), $GeSe_4$ (E_g^{CL} = 1.97 eV) and $Ge_{28}Sb_{12}Se_{60}$ (E_g^{CL} = 1.68 eV) are used. For Ga-Sb-Se co-sputtered films, the range of E_g^{CL} 1.35-1.92 eV and corresponding refractive index range of 3.34-2.47 is also decently covered, though the deposition rate of Ga_2Se_3 is significantly lower than that of Sb_2Se_3. In both ternary systems, the introduction of heavy antimony atoms is

responsible for the decrease of optical bandgap energy accompanied with corresponding increase of refractive index due to its high polarizability.

Sputtered Ge-Sb-Se-Te films, where the selenium is only partially altered by tellurium (10 and 15 at. %) relative to Se-rich Ge-Sb-Se films mentioned above, were also studied. Despite the fact that the surface roughness (RMS) of most of the prepared samples was only around ~0.3 ± 0.1 nm, thin films with higher tellurium content seem to be much grainier by means of topography. The studies of optical properties of sputtered films revealed expected drop of optical bandgap energy accompanied by increase of refractive index relative to tellurium-free Ge-Sb-Se films. The introduction of heavy tellurium provides the higher polarizability increasing the refractive index.

Nonlinear optical properties of co-sputtered ternary Ge-Sb-Se and Ga-Sb-Se and sputtered quaternary Ge-Sb-Se-Te films were studied by means of nonlinear refractive index (Kerr coefficient) n_2 and 2PA coefficient β. Numerical calculations of these coefficients were estimated by Sheik-Bahae's formalism [52] using the ellipsometry data (dispersion curves and optical bandgap energy E_g^{CL}). The balance between the refractive index and optical bandgap seems to be very important since the optical losses due to the large two-photon absorption can represent the limitation of a material for applications in nonlinear optics at desired wavelengths. For ternary Ge-Sb-Se and Ga-Sb-Se co-sputtered films, the value of optical bandgap energy of at least ~1.60 eV with corresponding refractive index at 1.55 μm around ~2.80 seems to be limit value for possible applications at telecommunication wavelength. This is in a suitable accordance with Tanaka who proposed materials with the Tauc gap of ≈ 1.80 eV as a best choice for nonlinear optical fibers [13]. The limiting calculated values of n_2 at 1.55 μm according this work are between ~1.13-1.34 × 10^{-17} m^2W^{-1}. These values are more than three orders of magnitude larger than that of silica (n_2 ~ 3 × 10^{-20} m^2W^{-1}) [56]. It should be noted that calculated values of n_2 using Sheik-Bahae's model for Ge-Sb-Se sputtered films are in a very good agreement with the literature.

Furthermore, high two-photon absorption may be expected in Ge-Sb-Se-Te films fabricated by sputtering. The alteration of selenium by tellurium in such system causes high decrease in optical bandgap which gives rise to high values of 2PA coefficient at 1.55 μm.

The study of local structure of fabricated films was performed by means of Raman spectroscopy data analysis. In germanium-rich thin films fabricated by co-sputtering, tetrahedral structure (*i.e.* [$GeSe_{4/2}$]) is expected where the $GeSe_2$ or $GeSe_4$ target is employed. In the case of films fabricated using the high electrical power on $GeSe_2$ target, Raman spectrum is dominated by two bands peaking at ~198 and ~216 cm^{-1} ascribed to symmetric stretching vibrations of heteropolar Ge–Se bonds in corner-sharing (A_1) and edge-sharing (accompanion mode, A_1^C) [$GeSe_{4/2}$] structural unit. The intensity of Raman band at ~216 cm^{-1} is much lower for films co-sputtered from $GeSe_4$ target indicating that the structure is predominantly governed by heteropolar Ge–Se bonds in corner-sharing [$GeSe_{4/2}$] units in selenium-rich films. Presence of Se–Se dimers and short selenium chains (Se_n) in Se-rich films is also considered. In germanium-rich films, the presence of Ge–Ge homopolar bonds can be identified at ~175 cm^{-1}. The intensity of this peak becomes more significant when selenium-deficient $Ge_{28}Sb_{12}Se_{60}$ target is used.

The structure of co-sputtered amorphous Ga-Sb-Se thin films is still not well understood. It is assumed that gallium with its electronic configuration of s^2p^1 is 4-fold coordinated in chalcogenide glasses creating the dative bond *via* interaction with *p* lone

pair of chalcogen atoms [57]. However, there is still lack of information for this system due to the certain facts such as limited glass-forming ability. For more precise analysis of the local structure of co-sputtered films density functional theory calculations may be valuable to predict and identify specific vibrational modes in this system. The addition of antimony in both Ge-Sb-Se and Ga-Sb-Se systems induces the evolvement of Sb–Se stretching vibration modes in [$SbSe_{3/2}$] pyramidal units.

Finally, in Ge-Sb-Se-Te, the substitution of selenium by tellurium relative to Te-free Ge-Sb-Se films, seems to induce the various mixtures of entities, where the atoms of selenium are partly replaced by tellurium. Such replacement seems to shift corresponding peaks of these entities towards lower wavenumbers. This observation is consistent with the effect of chalcogen-chalcogen substitution on the structure of Ge-S-Se glasses [58].

Photosensitivity studies were performed by means of prolonged irradiation by near-bandgap light with respect to the penetration depth of used light source. In order to minimize the effect of surface photo-oxidation, samples were placed in photo-kinetic cell with the pure argon atmosphere. In co-sputtered Ge-Sb-Se films, two opposite shifts of the fundamental short-wavelength absorption edge were observed. Specifically, photobleaching effect (PB) in germanium-rich films deposited from $GeSe_2$ and photodarkening (PD) in selenium-rich films deposited from $GeSe_4$. The increase of bandgap due to the PB expressed as ΔE_g^{CL} may be as high as 0.15 eV ($Ge_{32.5}Sb_{1.2}Se_{66.3}$). The largest magnitude of PD was present in $Ge_{14.0}Sb_{5.7}Se_{80.3}$ ($\Delta E_g^{CL} = -0.05$ eV). The reason for such observation may lie in the different structure of films co-sputtered from these targets. Photodarkening in amorphous selenium is well known phenomena [59]. Kumar *et al.* proposed that the PD in Ge-deficient Ge_xSe_{100-x} evaporated films is due to the photocrystallization of amorphous selenium when irradiated by 532 nm laser source (intensity of 500 $mW \cdot cm^{-1}$) on air [60]. Moreover, Ge-deficient films with the high selenium content are probably more prone to PD due to their underconstrained glass network structure. With increasing germanium content, the glass network becomes more constrained, so the magnitude of PD is supressed. Besides that, at high content of germanium in Ge-Sb-Se films, the presence of Ge–Ge homopolar bonds is probably unavoidable. Although it was not confirmed in this work, homo-to-heteropolar bond conversion usually takes part during the irradiation resulting in PB effect.

To the author's knowledge, the photosensitivity of amorphous co-sputtered Ga-Sb-Se films was performed for the first time. The effect of prolonged irradiation on the optical properties seems to be of same manner as in Ge-Sb-Se system deposited from $GeSe_2$, $Ge_{28}Sb_{12}Se_{60}$ and Sb_2Se_3 targets. The largest PB expressed as ΔE_g^{CL} was found in binary Ga_2Se_3, with the value of 0.10 eV. Increasing antimony content in both Ge-Sb-Se and Ga-Sb-Se tend to decrease the magnitude of PB in these films.

Unlike the changes in optical bandgap energy no clear trends can be justified in the photoinduced refractive index changes Δn (extracted from VASE data) in both Ge-Sb-Se and Ga-Sb-Se systems. The largest decrease for Ge-Sb-Se co-sputtered films was found in sample with composition $Ge_{27.7}Sb_{5.9}Se_{66.4}$ - the refractive index of this sample decreased by 0.04 on irradiation. On the other hand, the photoinduced increase of highest magnitude was observed for samples with compositions $Ge_{23.3}Sb_{16.0}Se_{60.7}$ (+ 0.04) and $Ga_{19.2}Sb_{17.5}Se_{63.3}$ (+0.03) from Ge-Sb-Se and Ga-Sb-Se system respectively.

The fabrication and characterization of sputtered Ge-Sb-Se-Te thin films in this work is considered to give a decent background for potential study of co-sputtered films within this system.

References

1. Zakery A., Elliott S.R. Optical properties and applications of chalcogenide glasses: a review. *Journal of Non-Crystalline Solids.* 2003;*330:*1-12.
2. Tanaka K., Shimakawa K. Chalcogenide glasses in Japan: A review on photoinduced phenomena. *physica status solidi (b).* 2009;*246:*1744-1757.
3. Sreeram A.N., Varshneya A.K., Swiler D.R. Microhardness and indentation toughness versus average coordination number in isostructural chalcogenide glass systems. *Journal of Non-Crystalline Solids.* 1991;*130:*225-235.
4. Tanaka K. Photoinduced processes in chalcogenide glasses. *Current Opinion in Solid State and Materials Science.* 1996;*1:*567-571.
5. Zallen R., The Physics of Amorphous Solids, Wiley, 2008,
6. Baudet E., Cardinaud C., Girard A., Rinnert E., Michel K., Bureau B., Nazabal V. Structural analysis of RF sputtered Ge-Sb-Se thin films by Raman and X-ray photoelectron spectroscopies. *Journal of Non-Crystalline Solids.* 2016;*444:*64-72.
7. Zakery A., Elliott S.R., Optical nonlinearities in chalcogenide glasses and their applications, Berlin ; New York Springer, 2007,
8. Savage J.A., Nielsen S. Chalcogenide glasses transmitting in the infrared between 1 and 20 μ — a state of the art review. *Infrared Physics.* 1965;*5:*195-204.
9. Baudet E., Sergent M., Němec P., Cardinaud C., Rinnert E., Michel K., Jouany L., Bureau B., Nazabal V. Experimental design approach for deposition optimization of RF sputtered chalcogenide thin films devoted to environmental optical sensors. *Scientific Reports.* 2017;*7:*3500.
10. Xu H., He Y., Wang X., Nie Q., Zhang P., Xu T., Dai S., Zhang X., Tao G. Preparation of Low-loss Ge15Ga10Te75 chalcogenide glass for far-IR optics applications. *Infrared Physics & Technology.* 2014;*65:*77-82.
11. Nazabal V., Jurdyc A.M., Němec P., Brandily-Anne M.L., Petit L., Richardson K., Vinatier P., Bousquet C., Cardinal T., Pechev S., Adam J.L. Amorphous Tm3+ doped sulfide thin films fabricated by sputtering. *Optical Materials.* 2010;*33:*220-226.
12. Schweizer T., Samson B.N., Moore R.C., Hewak D.W., Payne D.N. Rare-earth doped chalcogenide glass fibre laser. *Electronics Letters* (Vol. 33): Institution of Engineering and Technology, 1997, 414-416.
13. Tanaka K. Nonlinear optics in glasses: How can we analyze? *Journal of Physics and Chemistry of Solids.* 2007;*68:*896-900.
14. Eggleton B.J., Luther-Davies B., Richardson K. Chalcogenide photonics. *Nat Photon.* 2011;*5:*141-148.
15. Adam J.L., Zhang X., Chalcogenide Glasses: Preparation, Properties and Applications, Elsevier Science, 2014,
16. Alfano R.R., Shapiro S.L. Observation of Self-Phase Modulation and Small-Scale Filaments in Crystals and Glasses. *Physical Review Letters.* 1970;*24:*592-594.
17. Dai S., Wang Y., Peng X., Zhang P., Wang X., Xu Y. A Review of Mid-Infrared Supercontinuum Generation in Chalcogenide Glass Fibers. *Applied Sciences.* 2018;*8:*707.
18. Yu Y., Gai X., Ma P., Vu K., Yang Z., Wang R., Choi D.-Y., Madden S., Luther-Davies B. Experimental demonstration of linearly polarized 2 – 10 μm supercontinuum generation in a chalcogenide rib waveguide. *Optics Letters.* 2016;*41:*958-961.

19. Chauvet M., Fanjoux G., Huy K.P., Nazabal V., Charpentier F., Billeton T., Boudebs G., Cathelinaud M., Gorza S.-P. Kerr spatial solitons in chalcogenide waveguides. *Optics Letters.* 2009;*34:*1804-1806.
20. Andriesh A.M., Bertolotti M., Physics and applications of non-crystalline semiconductors in optoelectronics, Dordrecht ; Boston : Kluwer Academic, 1997,
21. Fritzsche H. The origin of reversible and irreversible photostructural changes in chalcogenide glasses. *Philosophical Magazine Part B.* 1993;*68:*561-572.
22. Halenkovič T., Němec P., Gutwirth J., Baudet E., Specht M., Gueguen Y., Sangleboeuf J.-C., Nazabal V. Co-sputtered amorphous Ge-Sb-Se thin films: optical properties and structure. *SPIE Optics + Optoelectronics*: 2017.
23. Chen Y., Shen X., Wang R., Wang G., Dai S., Xu T., Nie Q. Optical and structural properties of Ge–Sb–Se thin films fabricated by sputtering and thermal evaporation. *Journal of Alloys and Compounds.* 2013;*548:*155-160.
24. Šútorová K., Prokeš L., Nazabal V., Baudet E., Havel J., Němec P. Laser Desorption Ionization Time-of-Flight Mass Spectrometry of Glasses and Amorphous Films from Ge–As–Se System. *Journal of the American Ceramic Society.* 2016;*99:*3594-3599.
25. Halenkovič T., Gutwirth J., Němec P., Baudet E., Specht M., Gueguen Y., Sangleboeuf J.-C., Nazabal V. Amorphous Ge- Sb- Se thin films fabricated by co-sputtering: Properties and photosensitivity. *Journal of the American Ceramic Society.* 2018;*101:*2877-2887.
26. Němec P., Olivier M., Baudet E., Kalendová A., Benda P., Nazabal V. Optical properties of (GeSe2)100−x(Sb2Se3)x glasses in near- and middle-infrared spectral regions. *Materials Research Bulletin.* 2014;*51:*176-179.
27. Chen L.Y., Chen F.F., Dai S.X., Tao G.M., Yan L.H., Shen X., Ma H.L., Zhang X.H., Xu Y.S. Third-order nonlinearity in Ge-Sb-Se glasses at mid-infrared wavelengths. *Materials Research Bulletin.* 2015;*70:*204-208.
28. Olivier M., Tchahame J.C., Němec P., Chauvet M., Besse V., Cassagne C., Boudebs G., Renversez G., Boidin R., Baudet E., Nazabal V. Structure, nonlinear properties, and photosensitivity of (GeSe2)100-x(Sb2Se3)x glasses. *Optical Materials Express.* 2014;*4:*525-540.
29. Wei W.-H., Wang R.-P., Shen X., Fang L., Luther-Davies B. Correlation between Structural and Physical Properties in Ge–Sb–Se Glasses. *The Journal of Physical Chemistry C.* 2013;*117:*16571-16576.
30. Lecomte A., Nazabal V., Le Coq D., Calvez L. Ge-free chalcogenide glasses based on Ga-Sb-Se and their stabilization by iodine incorporation. *Journal of Non-Crystalline Solids.* 2018;*481:*543-547.
31. Lu Y., Song S., Shen X., Wang G., Wu L., Song Z., Liu B., Dai S. Phase change characteristics of Sb-rich Ga–Sb–Se materials. *Journal of Alloys and Compounds.* 2014;*586:*669-673.
32. Sharma N., Sharda S., Katyal S.C., Sharma V., Sharma P. Effect of Te on linear and non-linear optical properties of new quaternary Ge-Se-Sb-Te chalcogenide glasses. *Electronic Materials Letters.* 2014;*10:*101-106.
33. Lin L., Wang G., Shen X., Dai S., Xu T., Nie Q. Photo-induced structural changes in Ge-Sb-Se films. *Infrared Physics & Technology.* 2017;*81:*59-63.

34. Wang H., Wang G., Shi D., Shen X., Lu Y., Nie Q. Compositional dependence of crystallization and structural stability in Ge–Sb–Se chalcogenide films. *Journal of Non-Crystalline Solids.* 2016;*453:*108-112.
35. Chen F., Zhang Z., Wang Y., Nie Q., Shen X., Dai S. Optical properties of amorphous In-doped GeSe2 films for all-optical applications. *Infrared Physics & Technology.* 2015;*69:*32-35.
36. Cho J.-Y., Kim D., Park Y.-J., Yang T.-Y., Lee Y.-Y., Joo Y.-C. The phase-change kinetics of amorphous Ge2Sb2Te5 and device characteristics investigated by thin-film mechanics. *Acta Materialia.* 2015;*94:*143-151.
37. Park T.-J., Choi S.-Y., Kang M.-J. Phase transition characteristics of Bi/Sn doped Ge2Sb2Te5thin film for PRAM application. *Thin Solid Films.* 2007;*515:*5049-5053.
38. Zheng Y.-X., Zhang R.-J., Chen L.-Y. Ellipsometry and Its Applications in Stoichiometry. In A. Innocenti and N. Kamarulzaman (eds), *Stoichiometry and Materials Science - When Numbers Matter*, 2012.
39. Losurdo M., Bergmair M., Bruno G., Cattelan D., Cobet C., de Martino A., Fleischer K., Dohcevic-Mitrovic Z., Esser N., Galliet M., Gajic R., Hemzal D., Hingerl K., Humlicek J., Ossikovski R., Popovic Z.V., Saxl O. Spectroscopic ellipsometry and polarimetry for materials and systems analysis at the nanometer scale: state-of-the-art, potential, and perspectives. *Journal of Nanoparticle Research.* 2009;*11:*1521-1554.
40. Hölscher H., Schwarz U.D. Theory of amplitude modulation atomic force microscopy with and without Q-Control. *International Journal of Non-Linear Mechanics.* 2007;*42:*608-625.
41. Voigtländer B., Scanning Probe Microscopy: Atomic Force Microscopy and Scanning Tunneling Microscopy, Springer Berlin Heidelberg, 2015,
42. Kuriakose T., Baudet E., Halenkovič T., Elsawy M.M.R., Němec P., Nazabal V., Renversez G., Chauvet M. Measurement of ultrafast optical Kerr effect of Ge–Sb–Se chalcogenide slab waveguides by the beam self-trapping technique. *Optics Communications.* 2017;*403:*352-357.
43. Kuriakose T., Nazabal V., Renversez G., Baudet E., Němec P., Boidin R., Chauvet M. Beam self-action in planar chalcogenide waveguides. *SPIE Photonics Europe*: 2016.
44. Aitchison J.S., Hutchings D.C., Kang J.U., Stegeman G.I., Villeneuve A. The nonlinear optical properties of AlGaAs at the half band gap. *IEEE Journal of Quantum Electronics.* 1997;*33:*341-348.
45. Chen Z., Segev M., N. Christodoulides D. Optical spatial solitons: historical overview and recent advances. *Reports on Progress in Physics.* 2012;*75:*086401.
46. Kuriakose T., Halenkovic T., Elsawy M.M.R., Nemec P., Nazabal V., Renversez G., Chauvet M. Experimental demonstration of soliton-plasmon coupling in planar waveguides (Conference Presentation). *SPIE Photonics Europe*: 2018.
47. Tauc J., Amorphous and liquid semiconductors, London, New York, Plenum, 1974,
48. Afifi M.A., Bekheet A.E., El-Shair H.T., Zedan I.T. Determination and analysis of optical constants for Ga2Se3 films near absorption edge. *Physica B: Condensed Matter.* 2003;*325:*308-318.
49. Baudet E., Gutierrez-Arroyo A., Baillieul M., Charrier J., Němec P., Bodiou L., Lemaitre J., Rinnert E., Michel K., Bureau B., Adam J.L., Nazabal V. Development of

an evanescent optical integrated sensor in the mid-infrared for detection of pollution in groundwater or seawater. *Advanced Device Materials.* 2017;*3:*23-29.
50. Baillieul M., Halenkovič T., Gutierrez-Arrovo A.J., Baudet E., Rinnert E., Gutwirth J., Němec P., Charrier J., Bodiou L., Colas F., Boukerma K., Boussard C., Bureau B., Michel K., Nazabal V. Infrared-Sensor Based on Selenide Waveguide Devoted to Water Pollution. *20th International Conference on Transparent Optical Networks, ICTON 2018.* Bucharest, Romania: 2018.
51. Abdellaoui N., Starecki F., Boussard-Pledel C., Shpotyuk Y., Doualan J.L., Braud A., Baudet E., Nemec P., Cheviré F., Dussauze M., Bureau B., Camy P., Nazabal V. Tb3+ doped Ga5Ge20Sb10Se65-xTex (x = 0-37.5) chalcogenide glasses and fibers for MWIR and LWIR emissions. *Optical Materials Express.* 2018;*8:*2887-2900.
52. Sheik-Bahae M., Hagan D.J., Van Stryland E.W. Dispersion and band-gap scaling of the electronic Kerr effect in solids associated with two-photon absorption. *Physical Review Letters.* 1990;*65:*96-99.
53. Wang T., Gai X., Wei W., Wang R., Yang Z., Shen X., Madden S., Luther-Davies B. Systematic z-scan measurements of the third order nonlinearity of chalcogenide glasses. *Optical Materials Express.* 2014;*4:*1011-1022.
54. Tichá H., Tichý L. Semiempirical relation between Non-linear susceptibility (refractive index), Linear refractive index and Optical gap and its Application to Amorphous chalcogenides. *Journal of Optoelectronics and Advanced materials.* 2002;*4:*381-386.
55. Shuker R., Gammon R.W. Raman-Scattering Selection-Rule Breaking and the Density of States in Amorphous Materials. *Physical Review Letters.* 1970;*25:*222-225.
56. Boyd R.W., Nonlinear optics, Amsterdam ; Boston Academic Press, 2008,
57. Tichý L., Tichá H. On the chemical threshold in chalcogenide glasses. *Materials Letters.* 1994;*21:*313-319.
58. Xuecai H., Guangying S., Yu L., Hongbo Y., Yonghua L. Structure and vibrational modes of Ge-S-Se glasses: Raman scattering and ab initio calculations. *Chalcogenide Letters.* 2012;*9:*465-474.
59. Tanaka K., Odajima A. Photodarkening in amorphous selenium. *Solid State Communications.* 1982;*43:*961-964.
60. Kumar R.R., Barik A.R., Vinod E.M., Bapna M., Sangunni K.S., Adarsh K.V. Crossover from photodarkening to photobleaching in a-GexSe100-x thin films. *Optics Letters.* 2013;*38:*1682-1684.

List of Student's Published Works

Papers in journals with impact factor

1. Boidin R., Halenkovič T., Nazabal V., Beneš L., Němec P. Pulsed laser deposited alumina thin films. *Ceramics International.* 2016;*42*:1177-1182.
2. Kuriakose T., Baudet E., Halenkovič T., Elsawy M.M.R., Němec P., Nazabal V., Renversez G., Chauvet M. Measurement of ultrafast optical Kerr effect of Ge-Sb-Se chalcogenide slab waveguides by the beam self-trapping technique. *Optics Communications.* 2017;*403:*352-357.

3. Mawale R., Ausekar M., Prokeš L., Nazabal V., Baudet E., Halenkovič T., Bouška M., Alberti M., Němec P., Havel J. Laser desorption ionization of As2Ch3 (Ch = S, Se, and Te) chalcogenides using quadrupole ion trap time-of-flight mass spectrometry: A comparative study. *J. Am. Soc. Mass Spectrom.* 2017;*28*:2569-2579.
4. Halenkovič T., Gutwirth J., Němec P., Baudet E., Specht M., Gueguen Y., Sangleboeuf J-C., Nazabal V. Amorphous Ge-Sb-Se thin films fabricated by co-sputtering: properties and photosensitivity. *J. Am. Ceram. Soc.* 2018;*101*:2877-2887.
5. Mandal D., Yadav R.K., Mondal A., Bera S.K., Aswin J.R., Němec P., Halenkovič T., Adarsh K.V. Intensity mediated change in the sign of ultrafast third-order nonlinear optical response in As2S2 thin films. *Opt. Lett.* 2018;*43*:4787-4790.
6. Mawale R., Halenkovič T., Bouška M., Gutwirth J., Nazabal V., Takáts V., Csík A., Havel J., Prokeš L., Němec P. Laser Desorption Ionization Time-of-Flight Mass Spectrometry of GexSe1-x Chalcogenide Glasses, Their Thin Films, and Ge:Se Mixtures. *J. Non-cryst. Solids (accepted)*.
7. Mawale R., Halenkovič T., Bouška M., Gutwirth J., Nazabal V., Bora P.L., Pečinka L., Prokeš L., Havel J., Němec P. Mass Spectrometric Investigation of Amorphous Ga-Sb-Se Thin Films, *Chem. – Eur. J. (manuscript under preparation)*.

Papers in journals without impact factor

8. Halenkovič T., Němec P., Gutwirth J., Baudet E., Specht M., Gueguen Y., Sangleboeuf J-C., Nazabal V. Co-sputtered amorphous Ge-Sb-Se thin films: Optical properties and structure. *Proc. SPIE 10228*, Nonlinear Optics and its Applications X, 1022803 (2017). DOI: 10.1117/12.2264726.

Presentations at conferences

9. Boidin R., Halenkovič T., Nazabal V., Beneš L., Němec P. Pulsed laser deposited alumina thin films. 13th International Symposium on Sputtering and Plasma Processes, July 8-10, 2015, Kyoto, Japan, Symposium Program, p. 15.
10. Halenkovič T., Gutwirth J., Baudet E., Němec P., Nazabal V. Optical and structural properties of amorphous Ge–Sb–Se thin films fabricated by co-sputtering. 8th International Conference on Nanomaterials - Research & Application (Nanocon), October 19-21, 2016, Brno, Czech Republic, List of Abstracts, p. 33.
11. Halenkovič T., Němec P., Gutwirth J., Baudet E., Specht M., Gueguen Y., Sangleboeuf J-C., Nazabal V. Co-sputtered amorphous Ge-Sb-Se thin films: Optical properties and structure. SPIE Optics + Optoelectronics 2017, April 24-27, 2017, Prague, Czech Republic, Technical program, p. 22.
12. Kuriakose T., Baudet E., Halenkovic T., Elsawy M.M.R, Němec P., Nazabal V., Renversez G., Chauvet M. MESURE DE L'EFFET KERR DANS DES GUIDES PLANS PAR ANALYSE DE FAISCEAUX AUTO-PIEGES. Journées Nationales d'Optique Guidée, July 4-6, 2017, Limoges, France.
13. Kuriakose T., Halenkovič T., Elsawy M.M.R., Němec P., Nazabal V., Renversez G., Chauvet M.: Experimental demonstration of soliton-plasmon coupling in planar waveguides. SPIE Photonics Europe, April 22-26, 2018, Strasbourg, France, Technical Programme, p. 122.

14. Mawale R.M., Ausekar M.V., Prokeš L., Nazabal V., Baudet E., Halenkovič T., Bouška M., Alberti M., Havel J., Němec P.: A comparative time-of-flight mass spectrometry study of As2Ch3 (Ch = S, Se, and Te) chalcogenides using laser ablation. 21st International Symposium on Non-Oxide and New Optical Glasses, June 17-21, 2018, Quebec, Canada, Symposium Program, p. 169.
15. Halenkovič T., Gutwirth J., Němec P., Baudet E., Cardinaud Ch., Nazabal V. Amorphous Ge-Sb-Se thin films fabricated by RF sputtering for photonic applications: properties and photosensitivity. 3rd International Conference on Advanced Functional Materials, August 3-5, 2018, San Francisco, USA, Conference Program, p. 32.
16. Halenkovič T., Gutwirth J., Nazabal V., Němec P. Co-sputtered Ge-Sb-Se thin films – nonlinear materials for photonics applications. E-MRS 2018 Fall Meeting, September 17-20, 2018, Warsaw, Poland, Conference Programme, p. 235.
17. Baillieul M., Halenkovič T., Gutierrez-Arrovo A. J., Baudet E., Rinnert E., Gutwirth J., Němec P., Charrier J., Bodiou L., Colas F., Boukerma K., Boussard C., Bureau B., Michel K., Nazabal V. Infrared-sensor based on selenide waveguide devoted to water pollution. International Conference on Transparent Optical Networks, July 1-5, 2018, Bucharest, Romania, Conference Programme. DOI: 10.1109/ICTON.2018.8473739.